Journal of Power Sources 187 (2009) 332–340

Contents lists available at ScienceDirect

Journal of Power Sources

journal homepage: www.elsevier.com/locate/jpowsour

A novel inorganic/organic composite membrane tailored by various organic silane coupling agents for use in direct methanol fuel cells

Tao Li, Yong Yang*

State Key Laboratory for Physical Chemistry of Solid Surfaces and Department of Chemistry, College of Chemistry and Chemical Engineering, Xiamen University, Xiamen, 361005, PR China

ARTICLE INFO

Article history:
Received 29 October 2008
Accepted 5 November 2008
Available online 18 November 2008

Keywords:
Direct methanol fuel cell
Nafion
Composite membrane
Amino group
Electrostatic interaction
Basicity

ABSTRACT

A series of organic silica/Nafion composite membranes has been prepared by using organic silane coupling agents (SCA) bearing different hydrophilic functional groups. The physico-chemical properties of the composite membranes have been characterized by electrochemical techniques, scanning electron microscopy (SEM), diffuse-reflection Fourier-transform infrared spectroscopy (DRFTIR), wide-angle X-ray diffraction (WAXRD), thermogravimetric analysis (TGA), and thermogravimetric mass spectrometry (TG-MS). It has been found that some organic silica/Nafion composite membranes modified by organic silane agents bearing amino groups exhibit extremely low methanol crossover and proton conductivity values, e.g., a composite membrane shows a proton conductivity that is about five orders of magnitude lower and a methanol permeability that is about three orders of magnitude lower than those of a Nafion117 membrane. However, under optimized conditions for controlling the basicity of the amino groups, we also obtained a composite membrane with 89% lower methanol permeability and 49% lower proton conductivity compared with Nafion117 membrane. The results clearly demonstrate that the diffusion of methanol and protons through the membrane can be controlled by adjusting the functional groups on the organic silica.

1. Introduction

The direct methanol fuel cell (DMFC) has attracted wide interest in recent years due to its high energy efficiency and environmental compatibility. Its fuel, methanol, which is liquid at room temperature, can be easily and safely stored and transported. In addition, the DMFC system is simple in design and can be operated without fuel reforming. Perfluorosulfonic acid (PFSA) membranes, such as Dupont's Nafion membrane, have been widely used as proton-exchange membranes (PEMs) in DMFCs. Because of the great strength of the C–F bond, the perfluoro backbone gives the material excellent chemical and thermal stabilities. In the presence of water, the terminal sulfonic acid groups of PFSA are hydrated to form ion clusters, which give rise to high proton conductivity, e.g., $\sigma_{H^+} = \sim 10^{-2}\,S\,cm^{-1}$ for Nafion117 at room temperature [1]. However, because of the good affinity of methanol molecules for water molecules, methanol can permeate from the anode to the cathode through this hydrophilic domain, and over 40% of the methanol can be wasted in DMFCs [2]. Methanol crossover leads to fuel loss and reduced cathode voltage and cell performance, and is thus one of the major problems that must be overcome in DMFC application.

In order to decrease methanol crossover in Nafion membranes, many attempts have been made to modify the membrane, for example by adding minerals, incorporating organic materials into the film, copolymerization, and so on [3–13]. Since porous SiO_2 is known to be a proton conductor [14], it has been a popular inorganic additive for forming various composite membranes with Nafion. As is well known, Mauritz et al. were the first to report a novel Nafion/silica hybrid membrane, which was made by carrying out the in situ acid-catalyzed sol–gel reaction of tetraethoxysilane (TEOS) to form silica inside a Nafion membrane [15]. They also developed the method to form Nafion/[ORganically MOdified SILicate (ORMOSIL)] hybrid membranes [16–21]. These further studies were mainly concerned with diethoxydimethylsilane (DEDMS) and mixtures thereof with TEOS [16–20], and employed IR spectroscopy [17], a fluorescent probe method [18], SAXS [19], and thermal and mechanical analysis methods [20]. It was found that the ORMOSIL structure in the PFSA could be controlled by adjusting the external TEOS:DEDMS ratio [17], and that on increasing the concentration of DEDMS the resulting ORMOSIL structures became more hydrophobic and flexible [18,20]. Thereafter, Mauritz and co-workers employed some other semi-organic co-monomers (SOC), such as TEOS–triethoxyvinylsilane (TEVS), TEOS–methyltriethoxysilane (MTES), and TEOS–phenyltriethoxysilane (PTES) combinations, and used ^{29}Si solid-state NMR spectroscopy to investigate the exact compositions of the ORMOSIL nanostructures that were inserted

* Corresponding author. Tel.: +86 592 2185753; fax: +86 592 2185753.
E-mail address: yyang@xmu.edu.cn (Y. Yang).

0378-7753/$ – see front matter © 2008 Elsevier B.V. All rights reserved.
doi:10.1016/j.jpowsour.2008.11.035

into the cluster domains of the Nafion [21]. However, they did not investigate the effect of ORMOSILs bearing different organic groups on the performances of the hybrid membranes that are used as polymer electrolytes in DMFCs. Savinell and co-workers employed Mauritz's method to prepare Nafion/silica hybrid membranes with TEOS. The silica content was varied between approximately 3 and 26 wt%, and the hybrid membranes were separately evaluated for their proton conductivities [3] and methanol permeabilities [4]. Kim et al. used TEOS, TEVS, DEDMS, diethoxydiphenylsilane (DEDPS), and mixtures thereof as organic silane agents to form Nafion/ORMOSIL hybrid membranes [7]. By controlling the number of alkoxy groups and the type of organic group, they investigated the effects of hydrophilicity, interconnectivity, and compatibility of the ORMOSIL phase on the proton conductivities and methanol permeabilities of the composite membranes. However, they also did not discuss the effects of specific organic groups on the properties of the polymer membranes, and indeed all of the organic silane agents that they chose had relatively hydrophobic organic groups. Li et al. and Ren et al. used a casting method to form organic silica/Nafion composite membranes with diphenyldimethoxysilane (DDS) [11], TEOS, or mercaptopropylmethyldimethoxysilane (MPMDMS) [12], and to increase the $-SO_3H$ group content in the hybrid membranes they sulfonated DDS or oxidized the mercaptan groups to sulfonic acid groups. Lavorgna et al. [13] also used a mixture of TEOS and γ-propyl mercaptotriethoxysilane (MPTMS) as a precursor to form organic silica/Nafion composite membranes by a sol–gel method, and then oxidized the –SH groups in the siloxane network to $-SO_3H$ groups to increase the proton concentration in the membrane.

As noted above, there have been very few publications that have systematically dealt with the effects of different organic groups of the organic silica component on methanol/proton transportation in Nafion/organic silica composite membranes. In addition, it is well known that both protons and methanol primarily diffuse through the hydrophilic water-rich domains in Nafion [22,23]. Therefore, ORMOSILs bearing relatively hydrophilic organic groups may impact more on methanol/proton transportation than those bearing hydrophobic organic groups, and so the effects of relatively hydrophilic organic groups, such as ester or amino groups, on the performances of the composite membranes need further clarification.

For this purpose, in this work, we have prepared Nafion/organic silica composite membranes using a variety of organic silane coupling agents (SCA) bearing different hydrophilic functional groups. We have found that the amino groups can serve to "anchor" the sulfonic acid groups due to the strong electrostatic interaction between them. When the amino groups are combined with sulfonic acid groups, the condensation of the silane coupling agent might only be possible in a certain direction, akin to reaction in the presence of a "template", and this results in a significant decrease in the methanol permeability of the composite membrane. As far as we are aware, there has not hitherto been any report that has dealt directly with methanol/proton transportation in organic silica/Nafion composite membranes modified by organic silane agents bearing amino groups. Moreover, we also found that by controlling the basicity of the amino group the performance of the composite membrane could also be controlled. To the best of our knowledge, this phenomenon has likewise not been reported on previously.

2. Experimental

2.1. Materials

All of the organic silane coupling agents were purchased from Guotai-Huarong New Materials Co. Ltd. (China). The membranes used in this work were Nafion117 (Dupont, USA). Sulfuric acid (98 wt%), hydrogen peroxide (30 wt%), and HPLC grade methanol were purchased from the Sinopharm Chemical Reagent Co. Ltd. (China) and were used as received.

2.2. Preparation of Nafion/organic silica composite membranes

The Nafion117 membranes were pre-treated according to the standard procedure: 60 min in 5 wt% aqueous H_2O_2 solution at 80 °C, 60 min in deionized water at 80 °C, 60 min in 1 M H_2SO_4 solution at 80 °C, and finally rinsing several times with deionized water at 80 °C. After this pre-treatment, the membranes were dried in a vacuum oven at 80 °C for 24 h and then weighed.

The dry samples were fully hydrated in deionized water or methanol/water solution for at least 24 h. The silane coupling agent was mixed with methanol in a volume ratio of 1:5–1:20 (depending on the specific functional groups), and then the hydrated Nafion117 membranes were soaked in the solution for 5–10 min. The samples were then removed from the solution, quickly washed with methanol, dried in a vacuum oven at 80 °C for 24 h, and weighed (e.g., a Nafion117 sample was first hydrated in deionized water, and was then immersed in a 17% solution of 3-mercaptopropyltrimethoxysilane in methanol for 5 min, which resulted in a composite membrane that contained ∼3.6 wt% of organic silica). To permit comparison of the effects of different functional groups on the properties of composite membranes, all of the prepared composite membranes had approximate organic silica contents of ∼3.50 wt%.

As silane coupling agents, we first used 3-mercaptopropyltrimethoxysilane (1#SCA), 3-methacryloxypropyltrimethoxysilane (2#SCA), and 3-(2-aminoethyl)aminopropyltriethoxysilane (3#SCA), and the hybrid membranes formed were denoted as SILCPM1, SILCPM2, and SILCPM3, respectively. A further modified agent, 3-ureidopropyltriethoxysilane (4#SCA), was then chosen to study the effects of the basicity of the amino group on the properties of the composite membrane, and the hybrid membrane formed was named as SILCPM4. All of the composite membranes were fully hydrated in deionized water prior to measurements of methanol permeability and proton conductivity.

2.3. Measurement of methanol permeability

A 60 mL two-compartment PTFE cell was used to investigate the methanol permeability of the membranes at room temperature (∼25 °C), and all of other characterizations were carried out at this temperature without special explanation. Compartment I was filled with an aqueous solution containing 1 M methanol and 0.5 M H_2SO_4; compartment II was filled with a 0.5 M H_2SO_4 solution. The membrane was clamped between the two compartments, the contents of both of which were stirred during the experiments. The methanol concentration in compartment II was monitored by chronoamperometry. A constant potential (0.9 V vs. a reference electrode) was applied for a pulse time of 10 s by means of an AUTOLAB (Holland Eco Chemie) instrument operating in galvanostatic mode. Pt foils served as working electrode (WE) and counter electrode (CE), while a saturated calomel electrode (SCE) was used as the reference electrode. The current detected obeys the Cottrell equation, which is given by:

$$I(t) = \frac{nFAD_0^{1/2}C_0}{(\pi t)^{1/2}} \quad (1)$$

where I is the recorded current, n is the number of electrons involved in the electro-oxidation, F is the Faraday constant, A is the surface area of the WE, D_0 is the methanol diffusion coefficient of the solution, C_0 is the concentration of methanol, and t is the pulse time. The slope of a plot of $I(t)$ vs. $t^{-1/2}$ is proportional to the methanol concentration. Thus, we measured the chronoamperom-

etry plots of a series of standard aqueous methanol solutions (i.e., 0.01 M, 0.02 M, 0.03 M, etc.), calculated the slopes of the plots of $I(t)$ vs. $t^{-1/2}$, and obtained a calibration curve giving the relationship between the slope and the methanol molar concentration. We could then obtain the permeated methanol concentration at any time, and the methanol permeability (P) could be calculated by Eq. (2):

$$C_{II}(t) = \frac{A}{V_{II}}\frac{DK}{L}C_I t \quad (2)$$

where C_{II} is the methanol concentration in compartment II, C_I is the methanol concentration in compartment I, A and L are the area and thickness of the membrane, D and K are the methanol diffusivity and the partition coefficient between the membrane and the adjacent solution, t is the permeation time, and V_{II} is the volume of the solution in compartment II. The product DK is the methanol permeability P.

2.4. Measurement of proton conductivity

The orthogonal conductivity of the membranes was measured using a four-probe DC technique described by Tricoli and coworkers [24,25]. The cell consisted of two compartments separated by a vertical membrane. Each compartment was filled with 0.5 M H_2SO_4 solution. Two platinum foils were used as electrodes and were placed in compartment I and compartment II, respectively. When a constant current (~20 mA cm^{-2}) was applied to these two platinum electrodes, the voltage drop was simultaneously measured between two calomel reference electrodes that were symmetrically arranged on either side of the vertical membrane and connected to a digital multimeter. The resistance of the membrane could then be obtained as the difference between the ohmic drop in the presence and in the absence of the membrane. We also varied the current and repeated the experiment several times to ensure the accuracy of the results. Finally, the proton conductivity σ could be calculated by using Eq. (3):

$$\sigma = \frac{L}{RA} \quad (3)$$

where L, R, and A are the thickness, the resistance, and the orthogonal area of the membrane, respectively.

2.5. Morphology of the composite membranes

Scanning electron microscopy (SEM) (Oxford Instruments, LEO1530) was used to observe the morphologies of membranes. Before the experiment, gold was sputtered on the surface of the membrane for 25 s in vacuum.

2.6. IR spectroscopy

Diffuse-reflection Fourier-transform infrared (DRFTIR) spectra of the composite membranes were collected in the wavenumber range from 650 to 4000 cm^{-1} on a Nicolet Avatar 360 FT-IR spectrometer equipped with a Cenranrus microscope and a liquid N_2 cooled MCT detector. All spectra presented in this work represent the average of 64 interferometric scans with a resolution of 4 cm^{-1} obtained using Ominc 6.0a software.

2.7. X-ray diffraction

The crystal framework of the composite membranes was investigated by means of an X-ray diffractometer (Panalytical X'pert) using CuK_α radiation over a 2θ range from 10 to 90°.

2.8. Thermal decomposition of the membranes

The thermal stabilities and the decomposition products of the composite membranes were analyzed by TG and thermogravimetric mass spectrometry (TG-MS) using a Netzsch STA 409 PC TG-DTA interfaced to a 403C Aëolos® GC/MS. The samples (~10 mg) were heated from 25 to 600 °C at a scanning rate of 10 °C min^{-1} under a flow of N_2, and the gaseous decomposition products were introduced directly into the MS unit via a silica capillary.

3. Results and discussion

3.1. Preparation of composite membranes and measurement of methanol permeability and proton conductivity

Fig. 1 shows the methanol permeation rate curves for Nafion117 and the composite membranes, and the methanol permeabilities as well as the proton conductivities of the membranes are shown in Table 1. As can be seen in Fig. 1 and Table 1, all of the SILCPM membranes showed lower methanol permeability (P) and proton conductivity (σ) than Nafion117. Among them, SILCPM1 and SILCPM2 had similar P and σ; compared with Nafion117, the P values were decreased by about 50%, while σ was decreased by about 80% for SILCPM1 and 50% for SILCPM2. However, SILCPM3 showed extremely low values; its σ value was about five orders of magnitude lower and its P value was three orders of magnitude lower than those of the Nafion117 membrane. This might suggest a different reaction mechanism and microstructure between SILCPM1&2 and SILCPM3. We suspected that this big change was due to the presence of amino groups in 3#SCA. The amino groups could combine with the sulfonic acid groups of Nafion117 through electrostatic interactions. As a result, the condensation reaction would take place between these "attached" SCA molecules, leading to larger silica particles or crosslinking of the polyamine salt in the hydrophilic ion cluster region and the ion channels of Nafion. Such a structure would greatly block the transport of both methanol and protons. On the other hand, 1#SCA and 2#SCA do not pos-

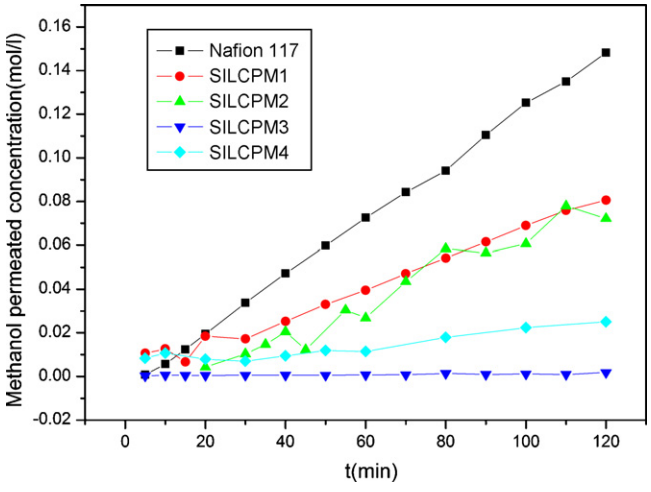

Fig. 1. Methanol permeation rate curves of Nafion117 and composite membranes at room temperature (~25 °C).

Table 1
Proton conductivities (Ω^{-1} cm^{-1}) and methanol permeability (cm^2 s^{-1}) of Nafion117 and SILCPM1–4 composite membranes at room temperature (~25 °C).

Sample	Nafion117	SILCPM1	SILCPM2	SILCPM3	SILCPM4
σ (S cm^{-1})	0.01639	2.085E-3	8.059E-3	1.837E-7	8.219E-3
P (cm^2 s^{-1})	3.08E-6	1.56E-6	1.83E-6	1.41E-8	3.40E-7

Table 2
The methanol-blocking-behavior of some different Nafion composite membranes.

Modified agent	Preparation method	Adulterated content (wt%)	Relative methanol permeability (vs. Nafion)	Reference
TEOS	Sol–gel	~20	~0.1	[4]
TEOS and DEDMS	Sol–gel	~45	~0.15	[7]
TEOS	Casting	5	0.55	[29]
Sulfonated DDS	Casting	25	0.26	[11]
TEOS and MPMDMS	Casting	5	0.5	[12]
Polypyrrole	In situ polymerization	3.5	0.381	[9]

sess groups that can combine with the sulfonic acid groups of Nafion117, and thus their condensation reactions would lack any ordering and would be likely to form smaller amorphous silica particles that merely increase the tortuosity of the methanol transport channels.

Park et al. have reported a Nafion/polypyrrole composite membrane that displayed improved mechanical and thermal stabilities as well as lower methanol crossover, and they ascribed these properties to the ionic interaction between the sulfonate groups of Nafion and the secondary ammonium groups of

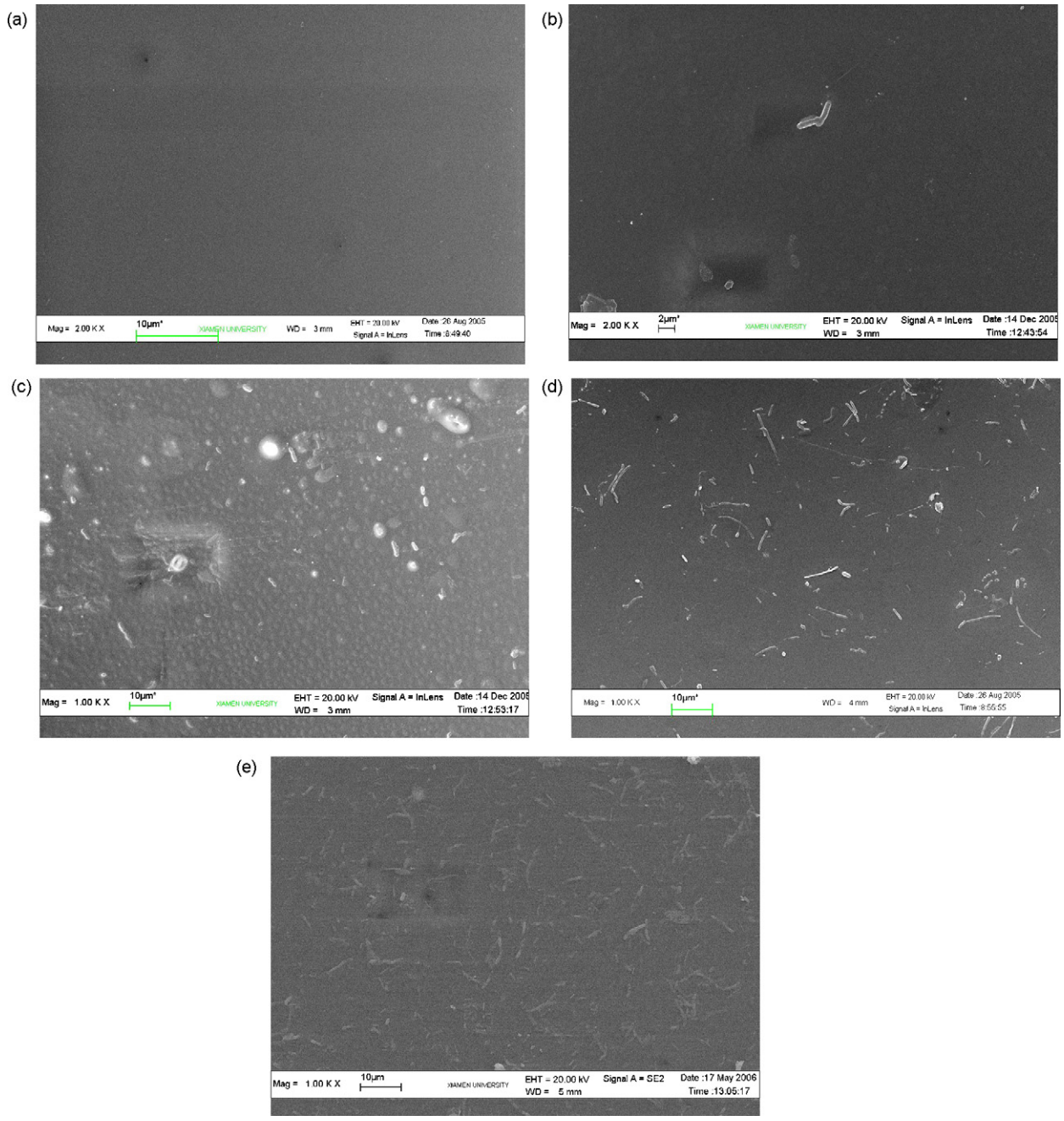

Fig. 2. SEM images of Nafion117 and Nafion117/silica composite membranes.

polypyrrole [8,9]. However, polymer additives within the hybrid membrane may act quite differently compared to inorganic ones. The Nafion/polypyrrole composite membrane showed a relative methanol permeability of 0.381 compared to that of Nafion with a polypyrrole content of 3.5 wt% [9]. However, our composite membrane SILCPM3, which has only ~3.5 wt% organic silica (the molecular weight of the repeat unit of polypyrrole is similar to the molecular weight of SiO_2), exhibited extremely low methanol permeability values, more than 200 times lower than that of Nafion117. In addition, it is known that the methanol permeability of silica/Nafion composite membranes normally decreases with increasing silica content. One of the Nafion/ORMOSIL hybrid membranes reported by Kim et al. [7] was made with TEOS and DEDMS; it exhibited ~85% lower methanol permeability than Nafion when it contained over 45 wt% of organic silica. Miyake et al. also reported a sol–gel derived Nafion/silica hybrid membrane with a silica content of ~20 wt%, which showed a methanol permeability one-tenth of that of Nafion [4]. In order to compare the methanol-blocking-behavior of the different Nafion composite membranes, the results from the above literature reports are also summarized in Table 2. It is reasonable to assume that the significant decrease in methanol permeability of our composite membrane SILCPM3 may be ascribed not only to the effect of the amino groups on the sulfonic acid groups, but also to the effect of the $-SO_3^-\ldots{}^+NH_3-$ ion pair on the formation of the organic silica phase that results from hydrolysis of the silane coupling agent in Nafion.

In order to confirm the proposed mechanism, besides performing further characterization experiments, we also introduced another SCA, 3-ureidopropyltriethoxysilane (4#SCA), which also bears amino groups. Because the carbonyl moiety in the $-CONH_2$ group is more electronegative than the methylene unit in the $-CH_2NH_2$ group, the amino group in 4#SCA has lower basicity. To investigate whether this new functional group could influence the interaction between the amino group and the sulfonic acid group, and hence the performance of the modified membrane, we measured the methanol permeability and proton conductivity of SILCPM4, and the results are also included in Fig. 1 and Table 1. From these results, it can be seen that SILCPM4 exhibited intermediate methanol permeability between SILCPM1&2 and SILCPM3. Compared with Nafion, its methanol permeability was decreased by 89%, while its proton conductivity was decreased by 49%. The intermediate properties of the SILCPM4 membrane fulfilled our expectation and further support our assumption. Moreover, the results testify that the performance of Nafion/organic silica composite membranes modified with organic silane agents bearing amino groups may be adjusted by controlling the basicity of the amino groups.

3.2. SEM results for Nafion117 and the composite membranes

Fig. 2a–e show the surface morphologies of unmodified Nafion117 and the composite membranes. Compared with Nafion, all of the hybrid membranes display organic silica particles on their surfaces. However, the surface of SILCPM1 appears to be almost as smooth as that of Nafion, which suggests a better compatibility between 1#SCA and Nafion. Although the SILCPM2–4 membranes appeared to have rough surfaces, in general they were uniform and homogeneous, and indeed all of the hybrid membranes were transparent. It is worthy of note that SILCPM3 showed a very similar surface morphology to that of SILCPM4, which might suggest a similar condensation reaction between 3#SCA and 4#SCA in hydrated Nafion, in accordance with our proposed mechanism.

3.3. Comparison of the IR spectra of the Nafion and composite membranes

DRFTIR measurements were carried out to investigate the functional groups of the newly formed organic silica phase in the hybrid membranes. Fig. 3 shows the DRFTIR spectra of dried Nafion117 and the composite membranes. The major peaks at ~1237 and ~1158 cm^{-1} may be attributed to the asymmetric and symmetric stretching vibrations of CF_2 in the fluorocarbon backbone, the absorption at ~1058 cm^{-1} is attributed to the symmetric stretching vibration of the $-SO_3^-$ groups, and the band at ~980 cm^{-1} is assigned to the symmetric C–O–C vibration [26]. Compared with Nafion117, the new absorption band that appears at 1731 cm^{-1} in the spectrum of the SILCPM2 membrane can be assigned to the stretching vibration of the –C=O group of the saturated fatty acid ester. The absorption band at 2277 cm^{-1} in the spectrum of the SILCPM3 membrane may be assigned to the asymmetric and symmetric stretching vibrations of NH_2^+, while the band at 1915 cm^{-1} is the characteristic absorption of NH_3^+. The SILCPM4 membrane also displayed a new absorption band at 1692 cm^{-1}, which could be assigned to the vibration of the C=O bond in the urea group, and the shift to higher wavenumber of the band may be attributed to the induction effect of the NH_3^+ group formed [27].

Because of the low organic silica content, only the intense absorption bands of the functional groups can be seen in the DRFTIR spectra (and SILCPM1 does not give rise to any new absorption bands compared with Nafion117). In addition, we did not

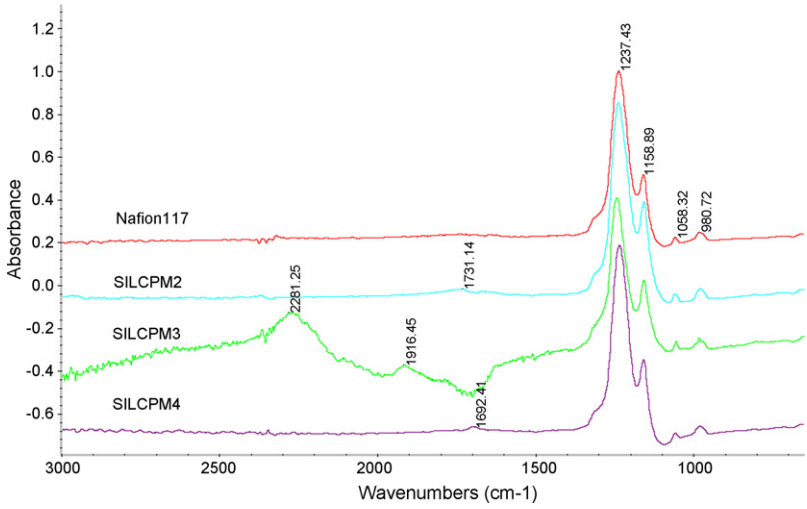

Fig. 3. Diffuse-reflection Fourier-transform infrared (DRFTIR) spectra of Nafion117 and Nafion117/silica composite membranes.

observe the asymmetric stretching vibration of Si–O–Si groups at 1074 cm^{-1}, which was reported by Mauritz [28] and Jiang et al. [29]. This may be attributed not only to the low organic silica content in our membrane system, but also to the different IR experiment mode used in our study. Nevertheless, these DRFTIR results clearly demonstrated the effectiveness of the modification reactions.

3.4. Wide-angle XRD patterns of Nafion117 and the composite membranes

The structure of a film, especially its degree of crystallinity, can be investigated by wide-angle X-ray diffraction (WAXRD) experiments. Fig. 4 shows the wide-angle X-ray diffraction patterns of dried Nafion117 and the Nafion/organic silica composite membranes. According to Moore and Martin [30] and Gierke et al. [31], Nafion samples display a broad diffraction feature at $2\theta = 12–22^\circ$, which results from a convolution of amorphous ($2\theta = 16^\circ$) and crystalline ($2\theta = 17.5^\circ$) scattering of the polyfluorocarbon chains. Here, all of the membranes displayed similar XRD patterns, with the exception of SILCPM3, which showed a much smaller, broad diffraction, with a shift to lower Bragg angles. In addition, SILCPM3 also exhibited several sharp diffraction peaks, as a result of the ordered structure in the hybrid membrane, which could be ascribed to crosslinking polyamine salt or crystalline silica. As yet, the reason for the formation of such an ordered structure, and the conditions under which it forms, remain unclear and need further studies. From a peak profile analysis of the broad diffraction feature, more detailed information, such as crystallinity (the ratio between the areas of crystalline scattering and amorphous scattering), could be derived, as shown in Fig. 5 and Table 3. The composite membranes had lower crystallinity than Nafion117 (the diffraction peak of SILCPM3 could not be subjected to peak profile analysis). The results were consistent with those reported by Xing and co-workers [32], but were at variance with those in some other literature reports [33–36], which might be due to the different methods used to prepare the composite membranes.

Table 3
The crystallinity of Nafion117 and Nafion117/silica composite membranes.

Membrane	Crystallinity (%)
Nafion117	65.2
SILCPM1	39.3
SILCPM2	38.1
SILCPM4	20.4

The lower crystallinity of the composite membranes can be attributed to SCA molecules that hydrolyze in crystalline regions of Nafion and interrupt their continuity [32]. However, SILCPM3 showed obvious differences in its structural characteristics compared with the other membranes. This suggested that after the amino groups of 3#SCA had been "captured" by the sulfonic acid groups of the Nafion, the condensation reaction between these "attached" SCA molecules took place according to the distribution of the sulfonic acid groups in the Nafion, forming denser and larger organic silica particles in SILCPM3, which greatly disrupted the crystal phase of the Nafion. Furthermore, inspecting the calculated crystallinity data shown in Table 3, it can be seen that the SILCPM1 and SILCPM2 samples had very similar values, which were clearly higher than that of SILCPM4. The lower crystallinity of SILCPM4 suggests that 4#SCA had a stronger effect on the structure of the Nafion117 than 1#SCA and 2#SCA (because its amino groups could also combine with the sulfonic acid groups of the Nafion), but that the electronegativity of the C=O group weakened the interaction between the amino and sulfonic acid groups. Therefore, the intermediate crystallinity of SILCPM4 (the crystallinity value of SILCPM3 could be regarded as approximately 0) also supported our supposition. We also found that heat treatment had an effect on the degree

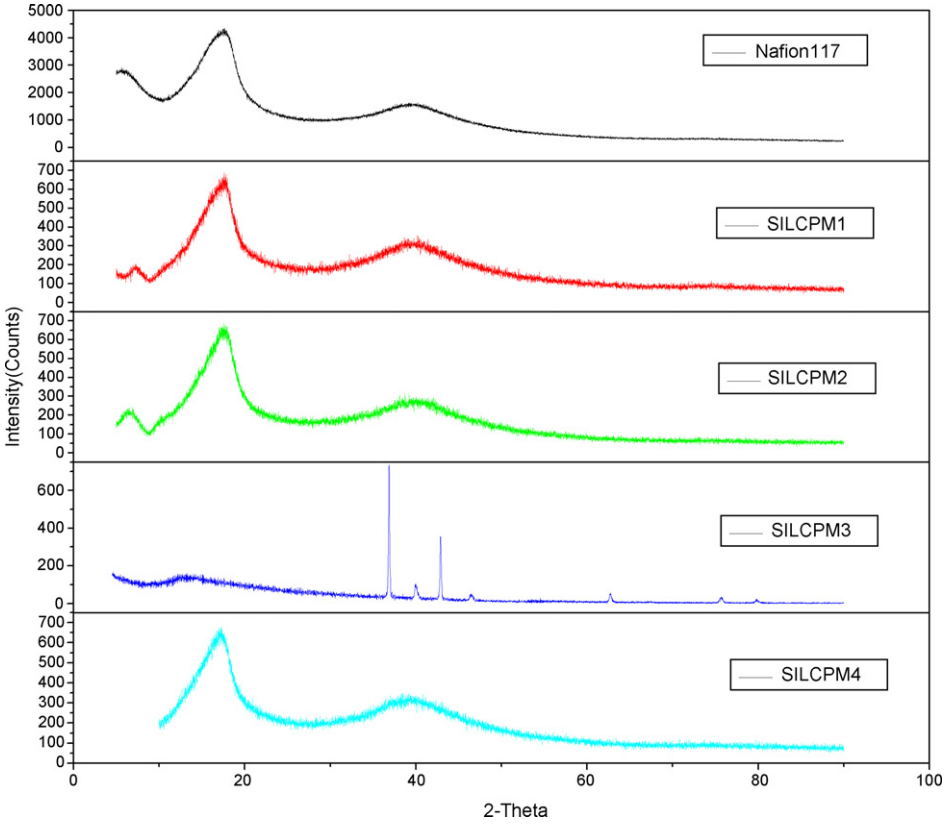

Fig. 4. The wide X-ray diffraction patterns of dried Nafion117 and Nafion/silica composite membranes.

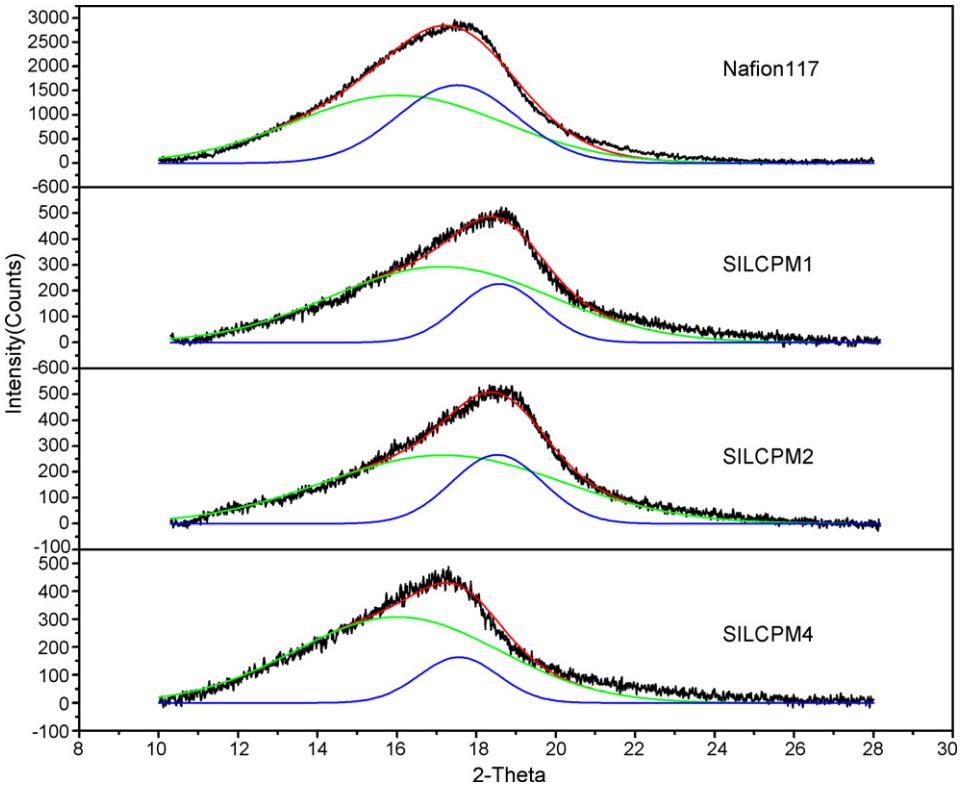

Fig. 5. The peak profile analysis of Nafion117 and SILCPM1–4.

of crystallinity [34,35]; the longer a membrane was dried at 80 °C in a vacuum oven, the higher the resultant crystallinity. Therefore, we ensured that all samples were subjected to the same heat treatment procedure prior to the WAXRD experiments.

3.5. Thermogravimetric analysis (TGA) and TG-MS results for the membranes

The results presented above strongly suggested that there was an ionic interaction between the amino groups of the SCA and the sulfonate groups of Nafion, and that this played an important role in the formation of the organic silica phase in hybrid membranes. To further prove such an effect, we investigated the thermal decomposition process of Nafion117 and the composite membranes by means of TG and TG-MS.

Fig. 6 shows the TG curves of dried Nafion117 and SILCPM1–4. It can be seen that SILCPM1–4 each had a similar residual weight percentage at 650 °C, which suggested that each had approximately the same organic silica content. The thermal degradation profiles of SILCPM1 and SILCPM2 were very similar. This can also be seen in the first-derivative TG curves shown in Fig. 7a. According to the work of Almeida and Kawano [37], the degradation process of Nafion117 membrane can be divided into three main stages. (Preliminary mass loss during the heating process from 25 to about 290 °C can be attributed mainly to the loss of absorbed water molecules or other impurities in the membrane.) The first stage (290–400 °C) is associated with a desulfonation process, the second stage (400–470 °C) relates to the decomposition of side chains, and the third stage (470–560 °C) relates to decomposition of the PTFE backbone. The peak of the second stage appears as a shoulder of the peak of the third stage. These three stages can clearly be seen in the degradation processes of SILCPM1&2, which are shown in Fig. 7a. However, as shown in Fig. 7b, only two stages appeared in the first-derivative TG curve of the SILCPM3 membrane. It was also found that the second stage peak of the SILCPM4 composite membrane was superimposed on the third stage peak, making it difficult to be distinguished, and hence the decomposition process of SILCPM4 seemed to be similar to that of SILCPM3. In addition, it is worthy of note that the temperatures corresponding to the maximum slopes of the different decomposition stages in the TG curves conformed to some specific sequences for these membranes. For the desulfonation stage, the temperatures decreased in the order SILCPM3 > SILCPM4 > SILCPM1 = SILCPM2 > Nafion117; this sequence can be attributed to the interaction between the sulfonic acid groups of Nafion117 and surface groups of organic silica. 3#SCA and 4#SCA bear amino groups, and the formation of the Nafion $-SO_3^-\ldots{}^+NH_3-$ silica ionic pair could stabilize the C–S bond in Nafion, thereby resulting in a higher desulfonation temperature. However, the C=O function of $-CONH_2$ in 4#SCA

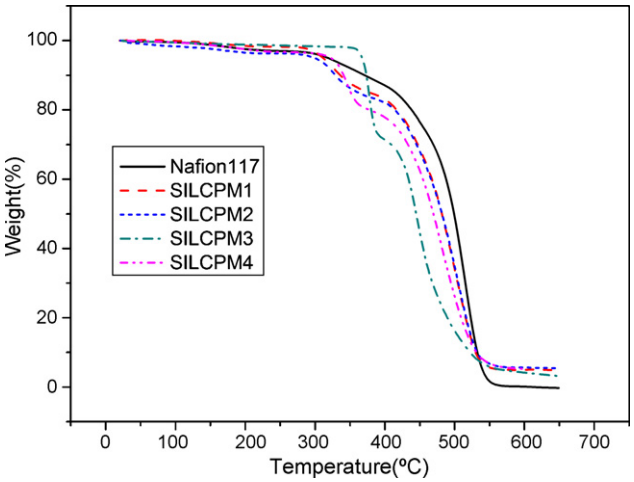

Fig. 6. The TG curves of dried Nafion117 and SILCPM1–4.

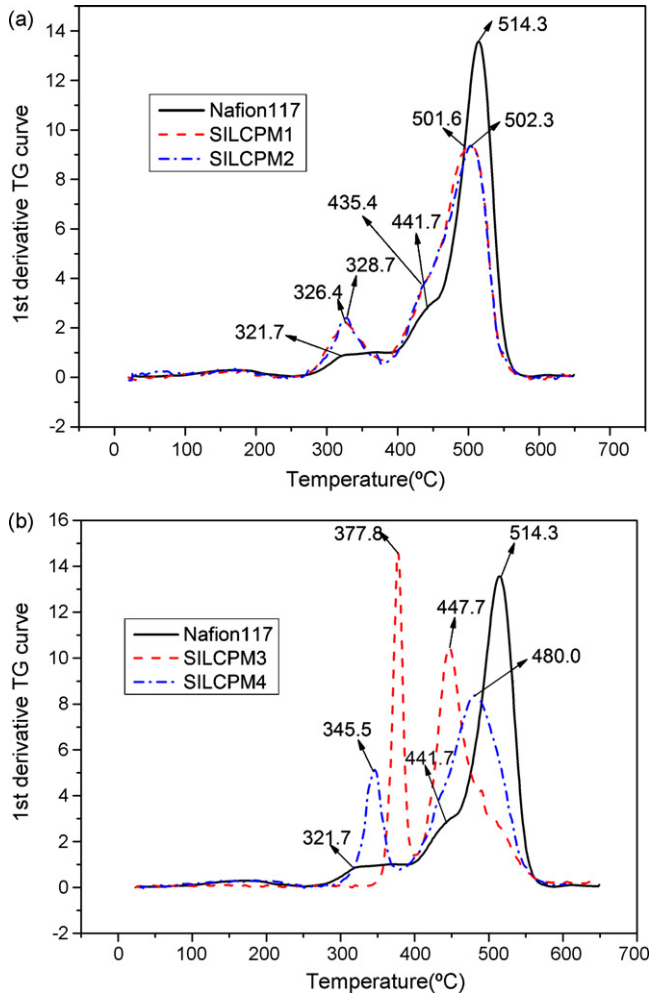

Fig. 7. The first-derivative of TG curves of (a) dried Nafion117 and SILCPM1&2, (b) dried Nafion117 and SILCPM3&4.

Table 4
Assignment of m/z peak in the thermal decomposition of Nafion117 and SILCPM4.

m/z	31	47	50	64	69
Fragment	CF^+	COF^+	CF_2^+	SO_2	CF_3^+

weakens this ionic pair, and so the desulfonation temperature of the SILCPM4 membrane is lower than that of SILCPM3. The organic groups in 1#SCA and 2# SCA (thiol groups and ester groups, respectively) have a much weaker effect (i.e., through van der Waals forces) on the sulfonic acid groups, which results in only a slightly higher desulfonation temperature than that of Nafion117. For the backbone decomposition stage, the temperature decreased in the order Nafion117 > SILCPM1 = SILCPM2 > SILCPM4 > SILCPM3, in good agreement with the crystallinity data for the membranes. The interaction between the sulfonic acid groups of Nafion117 and the organic groups on the silica indirectly decreased the crystallinity of the backbone and resulted in a lower backbone decomposition temperature [9]. However, the significantly depressed backbone decomposition temperature of SILCPM3 (more than 60 °C lower than that of Nafion117) demonstrated that the effect of the amino groups on the sulfonic acid groups was not solely responsible; the significant decrease was also due to the disruptive effect of the organic silica or crosslinking polyamine salt phase formed in SILCPM3 on the nonpolar backbone of Nafion117.

A typical TG-MS analysis of the decomposition process of a dried Nafion117 membrane is shown in Fig. 8 (lower panel). The peak at $m/z = 64$ (SO_2 fragment) centered at ~340 and 425 °C indicates the desulfonation process of Nafion117, and the peak at $m/z = 47$ (COF^+ fragment) centered at ~425 °C indicates the decomposition of the side chains. The backbone decomposition is reflected by the peaks at $m/z = 31$ (CF^+ fragment), 50 (CF_2^+ fragment), and 69 (CF_3^+ fragment), all of which are centered at ~510 °C. The fragments corresponding to each m/z value are summarized in Table 4. These mass loss peaks clearly demonstrated the three stages of the decomposition process of Nafion117, and the relevant temperatures were in good agreement with the TGA results. However, when Nafion117 was modified with 4#SCA, the TG-MS analysis changed dramati-

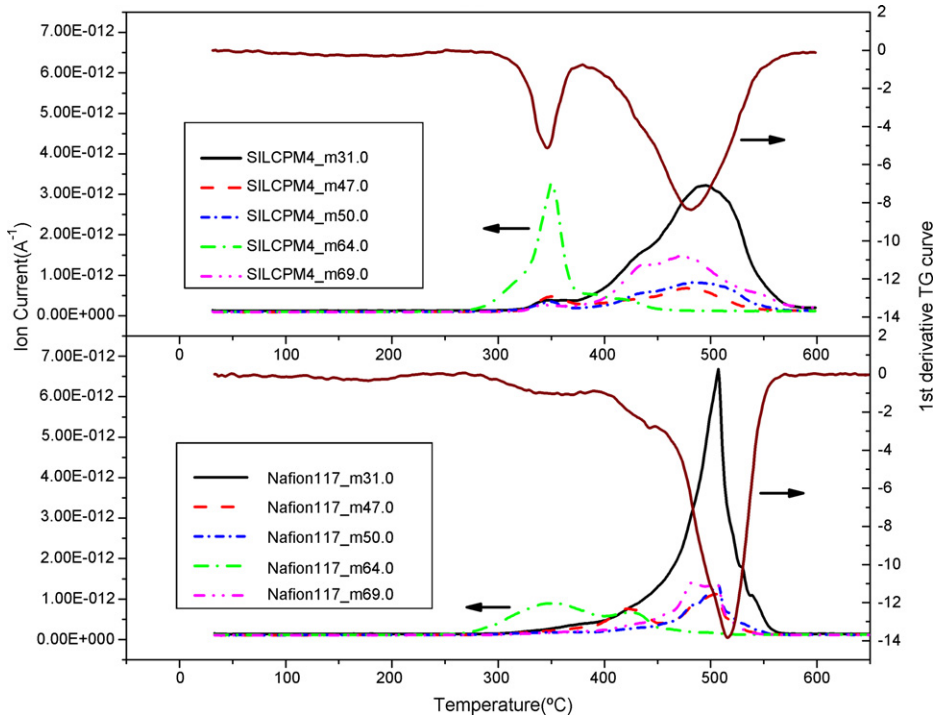

Fig. 8. The TG-MS results of dried Nafion117 (the lower panel) and SILCPM4 (the upper panel).

cally. As shown in the upper panel of Fig. 8, the peak at $m/z = 64$ for SILCPM4 was much sharper than in the case of Nafion117 and was only centered at ~350 °C, which indicated a rapid and relatively concentrated decomposition of the sulfonate groups. This was possibly due to a specific interaction between the sulfonate groups and the organic silica phase [38], and we attribute this specific interaction to the formation of Nafion $-SO_3^-\ldots{}^+NH_3-$ silica ionic pairs. Small portions of the ether side chains and C–F backbone were also observed to decompose at ~350 °C in the SILCPM4 membrane, and the mass loss peaks had a wider temperature range than in the case of Nafion117. All of these observations were indicative of easier decomposition of the side chains and backbone in the case of the SILCPM4 membrane, and this phenomenon may be due to the disruption of the crystalline phase of Nafion by introducing the organic silica into the membrane.

4. Conclusion

A series of Nafion/organic silica hybrid membranes has been prepared by using organic silane agents bearing different functional groups. An organic silica/Nafion composite membrane modified by an organic silane agent bearing aliphatic amino groups (SILCPM3) was found to exhibit extremely low proton conductivity and methanol permeability. In the light of former publications and characterization results, it is reasonable to assume that the significant decrease in methanol permeability of SILCPM3 may not only be ascribed to the effect of the amino groups on the sulfonic acid groups, but also to the effect of $-SO_3^-\ldots{}^+NH_3-$ ion pairs on the formation of the organic silica that results from hydrolysis of the silane coupling agent in the Nafion. Moreover, by controlling the electronegativity of the group connected to the amino group, the strength of the electrostatic interaction between the sulfonic acid groups of Nafion and the amino groups of the amino-based modifying reagents could be adjusted. Consequently, the condensation reaction of the SCA and the formation of the organic silica could also be controlled. Thus, among these composite membranes, SILCPM4 showed distinctive overall performance compared with Nafion117; its methanol permeability was decreased by 89%, and its proton conductivity was decreased by 49%. We intend to further investigate the effects of the group adjacent to the amino group with a view to optimizing the performance of the Nafion/organic silica hybrid membrane. Furthermore, there is also a need to investigate whether other characteristics of the organic group, such as steric effects, pK_a/pK_b, etc., also have an effect on the transportation of protons and methanol in Nafion/organic silica hybrid membranes.

Acknowledgement

This work was financially supported by the National Natural Science Foundation of China Grants (NO. 2043060, 29925310).

References

[1] J.J. Sumner, S.E. Creager, J.J. Ma, D.D. DesMarteau, J. Electrochem. Soc. 145 (1998) 107–110.
[2] D.H. Jung, S.Y. Cho, D.H. Peck, J. Power Sources 118 (2003) 205, and cited references.
[3] N. Miyake, J.S. Wainright, R.F. Savinell, J. Electrochem. Soc. 148 (8) (2001) A898–A904.
[4] N. Miyake, J.S. Wainright, R.F. Savinell, J. Electrochem. Soc. 148 (8) (2001) A905–A909.
[5] Z.G. Shao, X. Wang, I.M. Hsing, J. Membr. Sci. 210 (2002) 147–153.
[6] V. Tricoli, F. Nannetti, Electrochim. Acta 48 (2003) 2625–2633.
[7] Y.J. Kim, W.C. Choi, S.I. Woo, W.H. Hong, J. Membr. Sci. 238 (2004) 213–222.
[8] H.S. Park, Y.J. Kim, W.H. Hong, Y.S. Choi, H.K. Lee, Macromolecules 38 (2005) 2289–2295.
[9] H.S. Park, Y.J. Kim, W.H. Hong, H.K. Lee, J. Membr. Sci. 272 (2006) 28–36.
[10] S.P. Jang, Z.C. Liu, Z.Q. Tian, Adv. Mater. 18 (2006) 1068–1072.
[11] C.N. Li, G.Q. Sun, S.Z. Ren, et al., J. Membr. Sci. 272 (2006) 50–57.
[12] S.Z. Ren, G.Q. Sun, C.N. Li, et al., J. Membr. Sci. 282 (2006) 450–455.
[13] M. Lavorgna, L. Mascia, G. Mensitieri, et al., J. Membr. Sci. 294 (2007) 159–168.
[14] F.M. Vichi, M.T. Colomer, M.A. Anderson, Electrochem. Solid-State Lett. 2 (7) (1999) 313–326.
[15] K.A. Mauritz, R.F. Storey, C.K. Jones, Multiphase Polymer Materials: Blends and Ionomers, ACS Symposium Series No. 395, American Chemical Society, Washington, DC, 1989, p. 401.
[16] K.A. Mauritz, Mater. Sci. Eng. C6 (1998) 121–133.
[17] Q. Deng, R.B. Noore, K.A. Mauritz, Chem. Mater. 7 (1995) 2259–2268.
[18] Q. Deng, R.B. Noore, K.A. Mauritz, Chem. Mater. 9 (1997) 36–44.
[19] Q. Deng, K.M. Cable, R.B. Noore, K.A. Mauritz, J. Polym. Sci., Part B: Polym. Phys. 34 (1996) 1919–1923.
[20] Q. Deng, R.B. Noore, K.A. Mauritz, J. Appl. Polym. Sci. 68 (1998) 747–763.
[21] S.K. Young, W.L. Jarrett, K.A. Mauritz, Polymer 43 (2002) 2311–2320.
[22] J. Divisek, M. Eikerling, J. Electrochem. Soc. 145 (1998) 2677–2683.
[23] M.W. Verbrugge, J. Electrochem. Soc. 136 (1989) 417–423.
[24] V. Tricoli, J. Electrochem. Soc. 145 (1998) 3798–3801.
[25] V. Tricoli, N. Carretta, M. Bartolozzi, J. Electrochem. Soc. 147 (2000) 1286–1290.
[26] A. Gruger, A. Regis, T. Schmatko, P. Colomban, Vib. Spectrosc. 26 (2001) 215–225.
[27] J.G. Wu, The Techniques and Application of Fourier Transform Infrared Spectra (in Chinese), Scientific and Technical Documents publishing House, Beijing, 1994, pp. 601–607.
[28] K.A. Mauritz, Mater. Sci. Eng., C 6 (1998) 121–133.
[29] R.C. Jiang, H.R. Kunz, J.M. Fenton, J. Membr. Sci. 272 (2006) 116–124.
[30] R.B. Moore III, C.R. Martin, Macromolecules 21 (1988) 1334–1339.
[31] T.D. Gierke, G.E. Munn, F.C. Wilson, J. Polym. Sci. Phys. 19 (1981) 1687–1704.
[32] W.L. Xu, T.H. Lu, C.P. Liu, W. Xing, Electrochim. Acta 50 (2005) 3280–3285.
[33] P.L. Antonucci, A.S. Ario, P. Creti, E. Ramunni, V. Antonucci, Solid State Ionics 125 (1999) 431–437.
[34] P. Staiti, A.S. Arico, V. Baglio, F. Lufrano, E. Passalacqua, V. Antonucci, Solid State Ionics 145 (2001) 101–107.
[35] P. Dimitrova, K.A. Friedrich, U. Stimming, B. Vogt, Solid State Ionics 150 (2002) 115–122.
[36] Z.G. Shao, P. Joghee, I.M. Hsing, J. Membr. Sci. 229 (2004) 43–51.
[37] S.H. Almeida, Y. Kawano, J. Therm. Anal. Calorim. 58 (1999) 569–577.
[38] K.T. Adjemian, R. Dominey, et al., Chem. Mater. 18 (2006) 2238–2248.